

# Elimination of Porosity from Aluminum-Silicon Castings by Hot Isostatic Pressing

C.C. Chama

Specimens from two commercial aluminum-silicon casting alloys, with 0.060 and 0.100 maximum volume fractions of porosity, were hot isostatically pressed (HIPed) at 68.95 MPa and various combinations of temperature (500 to 560 °C) and time (15 to 120 min). Optical microscopy and scanning electron microscopy (SEM) were used to document the distribution of porosity before and after HIPing in addition to standard stereological techniques and high-precision density measurements. It was found that HIPing these alloys for at least 120 min led to the elimination of porosity. In all cases, there was a significant increase in density after HIPing.

## 1. Introduction

THE sources of porosity in castings are shrinkage and gas dissolution and subsequent exsolution, which occur during solidification. The gas responsible for the formation of porosity depends on the type of alloy being cast. In aluminum-base alloys, gas porosity is solely due to hydrogen.<sup>[1]</sup> During casting, for materials that do not expand on solidification, shrinkage accompanies the change in state from liquid metal to solid. Some of this shrinkage is uncompensated for and is retained as porosity. It is difficult to distinguish between porosity due to shrinkage or gas because the two types of porosity are formed simultaneously and at the same location.<sup>[2]</sup> Although the quantity of porosity formed in a casting can be minimized by adopting better foundry practices, complete avoidance of its formation is impossible. This is because of the limitations that are inherent in the casting processes.

There is evidence that some submicroscopic<sup>[3]</sup> and microscopic<sup>[4]</sup> porosity is eliminated by working and heat treatment. However, complete elimination of microporosity is impossible even after extensive working and heat treatment.<sup>[4]</sup> Hot isostatic pressing (HIPing) is the only process that has so far proved effective in healing porosity from a wide range of materials. It is a process that can allow for some flexibility in manufacturing procedures. This is because components not conforming to acceptable levels of quality can have properties improved by HIPing, a process that uses high temperatures in combination with large isostatic pressures to heal porosity. During HIPing, densification occurs, and the density increases toward the theoretical density because of the elimination of porosity. Phenomenological theories and models of HIPing are based primarily on investigations conducted on powder compacts. Densification models are based essentially on four processes: plastic flow,<sup>[5]</sup> power law creep,<sup>[6]</sup> lattice diffusion (Nabarro-Herring creep), and grain boundary diffusion (Coble creep).<sup>[7]</sup> During a HIPing cycle, all of the densification mechanisms may be operating. However, in most instances,

only one mechanism will be dominant in the elimination of porosity.

Even though HIPing technology has been in existence since the 1950s, it did not find wide industrial application for several years. However, in recent times, HIPing has become an increasingly important component of production in industry. This investigation arose from the consideration that, although pioneering work on HIPing has been conducted mostly on powder compacts, very little study has been performed on castings. Specifically, it has not been fully established if all forms of porosity present in castings can be eliminated by HIPing and as a consequence rejuvenate mechanical properties.

C.C. Chama, Department of Metallurgy and Mineral Processing, University of Zambia, Zambia.

Nomenclature	
$\gamma$ .....	Interfacial energy
$\rho$ .....	Relative density
$\Delta\rho$ .....	Densification
$\rho$ .....	Density of specimen
$\rho_a$ .....	Density of air
$\rho_i$ .....	Initial (pre-HIP) density
$\rho_f$ .....	Final (post-HIP) density
$\rho_t$ .....	Theoretical density
$\rho_w$ .....	Density of water
$D_{gb}$ .....	Grain boundary diffusion coefficient
$D_l$ .....	Lattice diffusion coefficient
$D_{o,gb}$ .....	Frequency factor for grain boundary diffusion
$D_{o,l}$ .....	Frequency factor for lattice diffusion
HIP.....	Hot isostatic press
$N_v$ .....	Number of pores per unit volume
$\Delta P$ .....	Pressure in a pore
$Q_{gb}$ .....	Activation energy for grain boundary diffusion
$Q_l$ .....	Activation energy for lattice diffusion
$R$ .....	Gas constant
$r$ .....	Pore radius
SEM.....	Scanning electron microscopy/microscope
$T$ .....	Temperature
$t$ .....	Time
$V_{ap}$ .....	Apparent volume fraction of porosity
$W_a$ .....	Mass of holder and specimen in air
$W_h$ .....	Mass of holder in air
$W_w$ .....	Mass of holder and specimen in water
$x_{gb}$ .....	Grain boundary diffusion distance
$x_l$ .....	Lattice diffusion distance

**Table 1** Compositions of Castings A and B

Casting	Si	Cu	Element, wt%		Sb	Al
			Mg	Fe		
A .....	7.12	0.05	0.16	0.29	0.06	bal
B .....	10.71	1.13	0.16	0.27	0.06	bal

**2. Experimental Procedures**

Specimens from two aluminum-silicon castings of compositions shown in Table 1 were HIPed at temperatures ranging from 500 to 560 °C and 68.95 MPa for 15 to 120 min. The first stage of the HIPing cycle involved heating the furnace to the set temperature. The second stage, pressurizing using argon gas, was initiated when the furnace was within a few degrees of the set temperature. Approximately 27 min was required to attain both the set temperature and pressure. The third stage involved holding the specimens at the set temperature and pressure for the desired (HIPing) time. When the holding time had elapsed, cooling and depressurizing of the furnace commenced.

Before HIPing, each specimen was examined for porosity by using an optical microscope and scanning electron microscopy (SEM). Information obtained in this manner was then compared to that obtained on the same specimen after HIPing. After HIPing, each specimen was cut into several sections, and these were then examined for porosity. Sectioning was necessary because HIPing only heals internal rather than surface porosity. In the examination of porosity, emphasis was placed on documenting the size distributions and measurement of volume fractions by point-counting techniques.<sup>[8]</sup> Furthermore, high-precision density measurements<sup>[9]</sup> were performed on each specimen before and after HIPing:

$$\rho^* = (\rho_w - \rho_a) \frac{(W_a - W_h)}{W_a - W_w} + \rho_a \quad [1]$$

To determine  $W_a$  and  $W_w$ , each specimen was put in a holder and then weighed in air and in distilled water. Before determining  $W_w$ , the specimen was put in a distilled water container, which was then put in an ultrasonic bath for a few minutes. Air trapped in surface-connected pores was expelled from the specimen during the residence of the specimen/distilled water container in the ultrasonic bath. Trapped air reduces the accuracy of measured densities. The following densities<sup>[10]</sup> were used in Eq 1:

$$\rho_a = 1.204 \text{ kg/m}^3 \quad [2]$$

$$\rho_w = 998 \text{ kg/m}^3 \quad [3]$$

Therefore:

$$\rho^* = \frac{996.796(W_a - W_h)}{W_a - W_w} + 1.204 \text{ kg/m}^3 \quad [4]$$

Equation 4 was used to calculate the density of each specimen after determining  $W_a$ ,  $W_h$ , and  $W_w$  on an electronic balance. The data obtained were then used to calculate densification and relative density as outlined below:

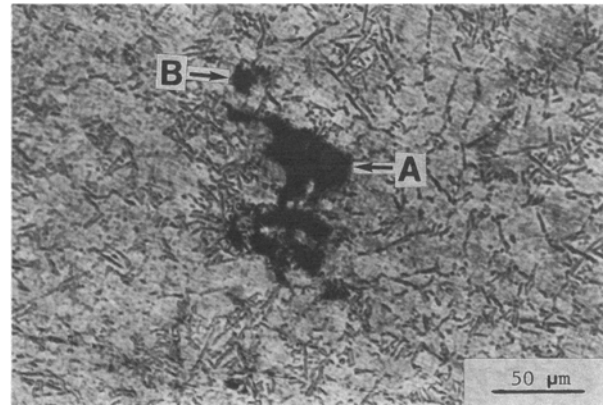


**Fig. 1** Microporosity and macroporosity in casting B in the as-cast state.

$$\Delta\rho = \frac{(\rho_f - \rho_i)}{\rho_i} 100\% \quad [5]$$

In addition, before HIPing:

$$\rho = \frac{\rho_i}{\rho_t} \quad [6]$$

And after HIPing:

$$\rho = \frac{\rho_f}{\rho_t} \quad [7]$$

Furthermore:

$$V_{ap} = 1 - \rho \quad [8]$$

**3. Results and Discussion**

**3.1 Microstructural and Macrostructural Examination of Porosity**

In the analysis of porosity, a distinction between microporosity and macroporosity has been made. Any pore less than about 100 μm in diameter or cross section has been designated as a micropore and that larger than 100 μm as a macropore. Before HIPing, there was a large difference in the volume fraction of macroporosity for the two castings. Specimens from casting A had a maximum volume fraction of macroporosity of 0.090. Few specimens from casting B contained macroporosity; the maximum volume of macroporosity was 0.050. The maximum volume fraction of microporosity was 0.010 for each casting.

As shown in the optical micrograph in Fig. 1, macroporosity (A) usually coexisted with microporosity (B). The micrograph in Fig. 1 was obtained from a polished but unetched specimen. Figure 2(a) shows the representative appearance of the most porous specimens obtained from these castings. As expected, larger macropores are located in the central portion of the casting, because this is the last region to solidify during casting. After HIPing, it was observed that macroporosity was extensively

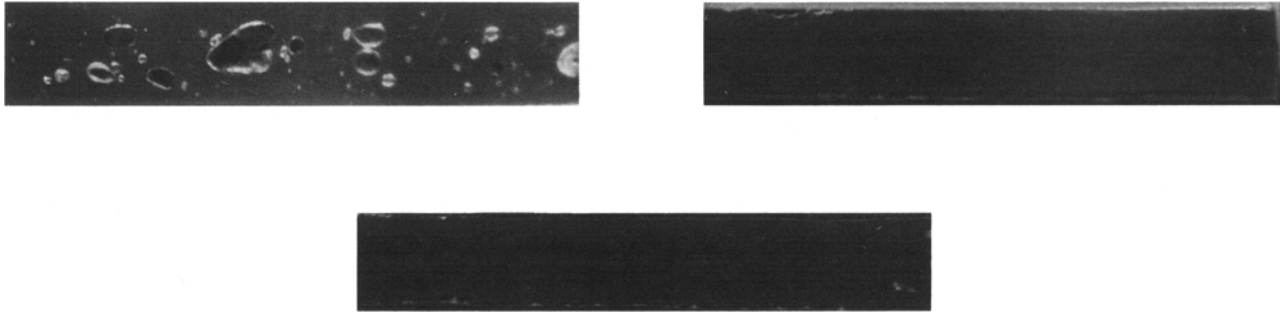


**Fig. 2** Macrostructure of casting A (a) before and (b) and (c) after HIPing at 68.95 MPa and 500 °C for 120 min.

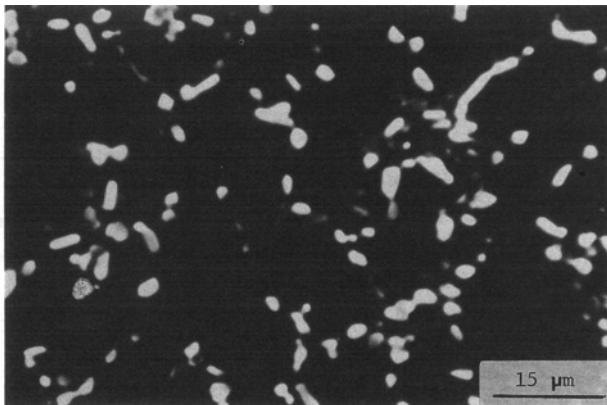


**Fig. 3** Casting A after HIPing at 68.95 MPa and 500 °C for 120 min.

eliminated from the castings, as shown in Fig. 2(b) and (c), which are sections obtained after cutting a HIPed specimen. During HIPing, there should be no change in the shape of a material, but a uniform reduction in size is expected due to the elimination of porosity. As is apparent from Fig. 2(b) and (c), there was no shape instability in the castings at these HIPing conditions. The SEM micrograph in Fig. 3 further confirms the absence of porosity in the HIPed materials.

### 3.2 Quantitative Evaluation of Porosity by Density Measurements

Accurate theoretical densities of castings A and B could not be determined by measurements, because it was impossible to verify that any specimen obtained from these castings was completely free of porosity. Therefore, theoretical densities for the castings were estimated on the basis of chemical composition by using a technique developed specifically for aluminum-base alloys.<sup>[11]</sup> The following estimated theoretical densities were determined as illustrated in Tables 2 and 3:

For casting A:

$$\rho_t = 2686 \text{ kg/m}^3 \quad [9]$$

For casting B:

$$\rho_t = 2690 \text{ kg/m}^3 \quad [10]$$

The dependence of densities on HIPing temperature is shown in Tables 4 and 5 for the specimens that were HIPed at 68.95 MPa for 120 min.

Due to the difficulty of finding specimens with similar pre-HIP densities, specimens from casting A with total volume fractions of porosity up to 0.050 were used for this particular investigation. After HIPing casting A, it was noted that the densification values were identical for all the temperatures shown in Table 4; all of the post-HIP densities were, however, below the estimated theoretical density (2686 kg/m<sup>3</sup>). The specimen that had been HIPed at 515 °C attained the least post-HIP density, probably due to the presence of surface-connected porosity or insufficient HIPing time. For casting B, substantial improvements in the densities were observed at all the HIPing temperatures shown in Table 5, but these were again below the theoretical density (2690 kg/m<sup>3</sup>). For both castings, the amount of densification was significant at all temperatures. The variation of density with HIPing time is shown in Table 6 for specimens that were HIPed at 68.95 MPa and 560 °C.

In the selection of specimens for these tests, emphasis was placed on choosing specimens with similar pre-HIP densities. It is clear that substantial densification occurred even for specimens that were HIPed for only 15 min. This indicates that, for a longer HIPing cycle, most of the densification occurs in the early stage. The nonuniform variation in densification as a function of HIPing time was probably due to the wide variability in the porosity contents of the specimens.

### 3.3 Stereological Analyses of the Distribution of Porosity

The actual volume fractions of porosity present in specimens were determined by measurements using point-counting techniques. On the other hand, the apparent volume fractions of porosity were calculated from Eq 8 after obtaining the densities from Eq 6 and 7. The actual and apparent volume fractions of porosity at different HIPing temperatures are shown in Tables 7 and 8.

There are some discrepancies between some actual and apparent values of volume fractions of porosity. These discrepancies can be explained as follows. Firstly, because in many cases

**Table 2 Calculation of Theoretical Density for Casting A**

Element	wt% of element in alloy	Calculated element concentration	Factor	Calculated element concentration × factor
Si .....	7.12	3.6	0.4292	1.545
Cu .....	0.05	0.02	0.1116	0.002
Mg .....	0.16	0.08	0.5522	0.044
Fe .....	0.29	0.15	0.1271	0.019
Sb .....	0.06	0.03	...	...
		3.88		1.610

**Note:** Sum of calculated element concentration = 3.88. Calculated element concentration for aluminum = 100 – 3.88 = 96.12. Calculated element concentration × factor for aluminum = 96.12 × 0.3705 = 35.612. Sum of calculated element concentration x factor = 1.610 + 35.612 = 37.222.  $\frac{100}{37.222} = 2.6865$ . Metric density =  $2.686 \times 10^3 = 2686 \text{ kg/m}^3$ .

**Table 3 Calculation of Theoretical Density for Casting B**

Element	wt% of element in alloy	Calculated element concentration	Factor	Calculated element concentration × factor
Si .....	10.71	5.4	0.4292	2.318
Cu .....	1.13	0.6	0.1116	0.067
Mg .....	0.16	0.08	0.5522	0.044
Fe .....	0.27	0.14	0.1271	0.018
Sb .....	0.06	0.03	...	...
		6.25		2.447

**Note:** Sum of calculated element concentration = 6.25. Calculated element concentration for aluminum = 100 – 6.25 = 93.75. Calculated element concentration × factor for aluminum = 93.75 × 0.3705 = 34.734. Sum of calculated element concentration x factor = 2.447 + 34.734 = 37.181.  $\frac{100}{37.181} = 2.6895$ . Metric density =  $2.690 \times 10^3 = 2690 \text{ kg/m}^3$ .

**Table 4 Effect of HIPing Temperature on Densities of Casting A Before and After HIPing at 68.95 MPa for 120 min**

HIPing temperature, °C	Pre-HIP		Post-HIP		Densification, %
	Density, kg/m <sup>3</sup>	Relative density	Density, kg/m <sup>3</sup>	Relative density	
500 .....	2509	0.934	2664	0.992	6.18
515 .....	2409	0.897	2570	0.957	6.68
532 .....	2526	0.940	2668	0.993	5.62
550 .....	2507	0.933	2638	0.982	5.22

the actual values are less than the apparent values, it is likely that by using the SEM some micropores were not resolved and are thus unaccounted for in the determination of the actual volume fractions of porosity. Secondly, the estimated theoretical densities for castings A and B of 2686 and 2690 kg/m<sup>3</sup>, respectively, may be too high. Thirdly, the apparent values are based on density measurements and therefore depend on all of the porosity (surface and internal) present in a specimen; the actual values are based on surface porosity alone. Despite these observations, the data in Tables 7 and 8 reveal that there was elimination of porosity after HIPing at a temperature of at least 500 °C. Similarly, Table 9 shows that a HIPing time of 120 min resulted in the virtual elimination of porosity.

Before HIPing, specimens usually contained significant porosity, as shown in Fig. 4(a). It is worth noting that the specimen in Fig. 4(a) contained more microporosity than macroporosity. After HIPing, even for a short time such as 30 min, there was extensive elimination of both microporosity and macroporosity (see Fig. 4b). Most of the pores were spherical. For size dis-

tributions such as those in Fig. 4(a) and (b), the value of  $2r$  was taken as the arithmetic mean of the upper and lower bounds of the size interval. For example, all of the pores in a bin between 100- and 200- $\mu\text{m}$  diameter were assigned a  $2r$  value of 150  $\mu\text{m}$ .

### 3.4 Mechanisms of Porosity Elimination

In the as-cast state, the room-temperature yield strengths of castings A and B are 86.02 and 122.48 MPa, respectively.<sup>[12]</sup> At 1000 °F ( $\approx 538$  °C), a yield stress of 800 psi ( $\approx 5.52$  MPa) has been determined on aluminum-silicon castings.<sup>[13]</sup> There is evidence that the yield stress of some castings with similar compositions to castings A and B decreases with increasing temperature.<sup>[14]</sup> Therefore, the yield strengths of castings A and B will be far below 86.02 and 122.48 MPa during HIPing because of the high temperature to which they are exposed. Because the high-temperature yield stress ( $\approx 5.52$  MPa) is much less than the HIPing pressure (68.95 MPa), it is very likely that

**Table 5 Effect of HIPing Temperature on Densities of Casting B Before and After HIPing at 68.95 MPa for 120 min**

HIPing temperature, °C	Pre-HIP		Post-HIP		Densification, %
	Density, kg/m <sup>3</sup>	Relative density	Density, kg/m <sup>3</sup>	Relative density	
500	2460	0.914	2646	0.984	7.56
515	2466	0.917	2652	0.986	7.54
532	2488	0.925	2626	0.976	5.55
550	2513	0.934	2604	0.968	3.62

**Table 6 Effect of HIPing Time on Densities of Casting A Before and After HIPing at 68.95 MPa and 560 °C**

HIPing time, min	Pre-HIP		Post-HIP		Densification, %
	Density, kg/m <sup>3</sup>	Relative density	Density, kg/m <sup>3</sup>	Relative density	
15	2468	0.919	2639	0.982	6.93
45	2482	0.924	2605	0.970	4.96
120	2488	0.926	2666	0.992	7.15

**Table 7 Effect of HIPing Temperature on Actual and Apparent Volume Fractions of Porosity in Casting A Before and After HIPing at 68.95 MPa for 120 min**

HIPing temperature, °C	Actual		Apparent	
	Pre-HIP	Post-HIP	Pre-HIP	Post-HIP
500	0.042	0.002	0.066	0.008
515	0.056	0.011	0.103	0.043
532	0.060	0.000	0.060	0.007
550	0.060	0.002	0.067	0.018

**Table 8 Effect of HIPing Temperature on Actual and Apparent Volume Fractions of Porosity in Casting B Before and After HIPing at 68.95 MPa for 120 min**

HIPing temperature, °C	Actual		Apparent	
	Pre-HIP	Post-HIP	Pre-HIP	Post-HIP
500	0.048	0.000	0.086	0.016
515	0.052	0.008	0.083	0.014
532	0.050	0.000	0.075	0.024
550	0.060	0.000	0.066	0.032

plastic flow had a very significant role in the elimination of porosity from castings A and B.

The influence of capillarity on the elimination of porosity was also evaluated. For porous materials such as castings A and B, the pressure inside a pore is:<sup>[15]</sup>

$$\Delta P \approx \frac{2\gamma}{r} \quad [11]$$

For aluminum,  $\gamma \approx 1 \text{ N/m}$ .<sup>[16]</sup> Therefore, Eq 11 can be written as:

$$\Delta P \approx \frac{2}{r} \text{ Pa} \quad [12]$$

For example, for pores with a  $2r$  value of  $1200 \mu\text{m}$  in Fig. 4(a),  $\Delta P$  is  $0.003 \text{ MPa}$ . Because the HIPing pressure ( $68.95 \text{ MPa}$ ) is much greater than the pressure inside the pores,  $0.003 \text{ MPa}$  in this particular case, it can be presumed that capillarity

did not play an important role in the elimination of porosity from castings A and B.

In addition, the role of grain boundary and lattice diffusion on porosity elimination was determined by considering diffusion distances. For lattice diffusion:

$$x_l = \sqrt{D_l t} \quad [13]$$

The matrix (darker phase in Fig. 3) for these castings is aluminum rich. Between  $450$  and  $650 \text{ }^\circ\text{C}$ , the self-diffusion of aluminum is:<sup>[17]</sup>

$$D_l = 1.71 \exp\left(\frac{-34,000 \text{ cal/mol}}{RT}\right) \text{ cm}^2/\text{s} \quad [14]$$

Equation 14 can be used to estimate the diffusivity of species such as vacancies and atoms in aluminum. At  $550 \text{ }^\circ\text{C}$ ,  $D_l$  is  $1.58 \times 10^{-9} \text{ cm}^2/\text{s}$ . According to Eq 13, the diffusion distance ( $x_l$ ) in a material that is HIPed at  $550 \text{ }^\circ\text{C}$  for  $60 \text{ min}$  is  $24 \mu\text{m}$ .

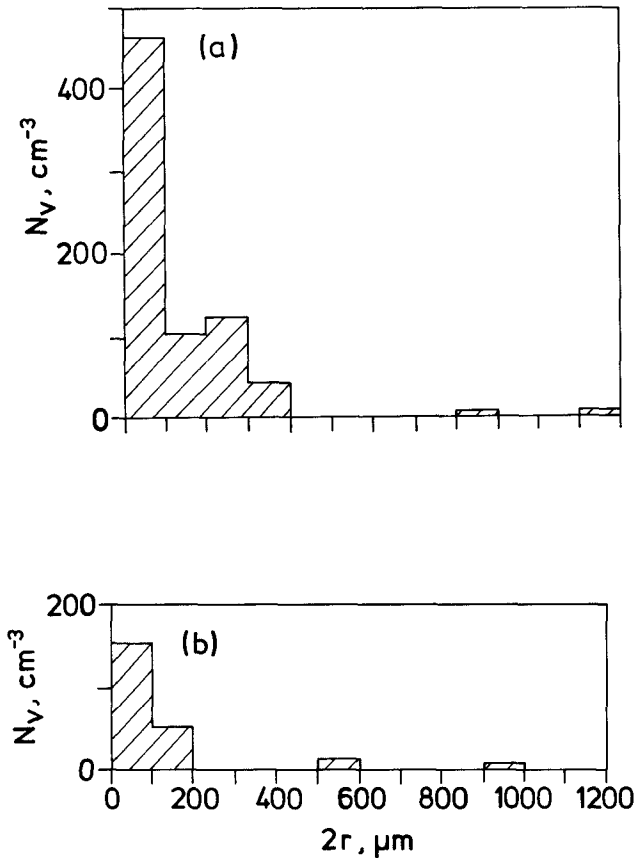


Fig. 4 Pore size distributions in casting A (a) before and (b) after HIPing at 68.95 MPa and 550 °C for 30 min.

Because the diffusion distance (24 μm) is very small compared to the minimum half thickness of the specimens (0.30 cm) used in this investigation, this implies that porosity elimination by lattice diffusion is insignificant. Similarly, for grain boundary diffusion:

$$x_{gb} = \sqrt{D_{gb} t} \quad [15]$$

In the absence of explicit grain boundary diffusion data for aluminum, the following approach can be adopted:

$$Q_{gb} = \frac{1}{2} Q_l \quad [16]$$

Assuming that:

$$D_{o,gb} \approx D_{o,l} \quad [17]$$

And using Eq 14 and 16:

$$D_{gb} \approx 1.71 \exp\left(\frac{-17,000 \text{ cal/mol}}{RT}\right) \text{ cm}^2/\text{s} \quad [18]$$

At 550 °C,  $D_{gb}$  is  $5.23 \times 10^{-5} \text{ cm}^2/\text{s}$ . Using Eq 15 for a HIPing time of 60 min, the diffusion distance ( $x_{gb}$ ) is 0.43 cm. The diffusion distance for grain boundary diffusion (0.43 cm) is larger than the minimum half thickness of the specimens,

Table 9 Effect of HIPing Time on Actual and Apparent Volume Fractions of Porosity in Casting A Before and After HIPing at 68.95 MPa and 560 °C

HIPing time, min	Actual		Apparent	
	Pre-HIP	Post-HIP	Pre-HIP	Post-HIP
15	0.088	0.050	0.081	0.017
45	0.069	0.056	0.076	0.030
120	0.042	0.000	0.074	0.007

which would indicate that Coble creep makes a significant contribution to the elimination of porosity when the HIPing time is 60 min. However, consideration of Table 6 reveals that densification occurs in a very short time. For example, a significant amount of densification occurs within 15 min of HIPing. In this period, the diffusion distance is 0.22 cm, which is again less than the minimum half thickness of the specimens. From all the above considerations, it would seem that the most probable dominant mechanism responsible for the elimination of porosity from castings A and B during HIPing was plastic flow.

#### 4. Conclusions

Hot isostatic pressing is an effective process for eliminating porosity from castings A and B. Extensive elimination of macroporosity and microporosity occurs in castings A and B when HIPed at 500 to 560 °C and 68.95 MPa for about 120 min. Significant densification of castings A and B occurs in the early stages of a HIPing cycle.

#### Acknowledgment

The author is grateful to the Department of Materials Science and Engineering at The Pennsylvania State University where this work was conducted.

#### References

1. P.M. Thomas and J.E. Gruzleski, Threshold Hydrogen for Pore Formation during the Solidification of Aluminum Alloys, *Metall. Trans. B*, Vol 9, 1978, p 139-141.
2. K. Kubo and R.D. Pehlke, Mathematical Modeling of Porosity Formation in Solidification, *Metall. Trans. B*, Vol 16, 1985, p 359-366.
3. E.J. Whittenberger and F.N. Rhines, Origin of Porosity in Castings of Magnesium-Aluminum and Other Alloys, *JOM*, Vol 4, 1952, p 409-420.
4. S.N. Singh and M.C. Flemings, Solution Kinetics of a Cast and Wrought High Strength Aluminum Alloy, *Trans. Metall. Soc. AIME*, Vol 245, 1969, p 1803-1809.
5. A.K. Kakar and A.C.D. Chaklader, Deformation Theory of Hot Pressing—Yield Criterion, *Trans. Metall. Soc. AIME*, Vol 242, 1968 p 1117-1120.
6. D.S. Wilkinson and M.F. Ashby, Pressure Sintering by Power Law Creep, *Acta Metall.*, Vol 23, 1975, p 1277-1285.
7. D.S. Wilkinson and M.F. Ashby, The Development of Pressure Sintering Maps, in *Materials Science Research*, Vol 10, G.C. Kuczynski, Ed., Plenum Press, 1975, p 473-492.

8. E.E. Underwood, *Quantitative Stereology*, Addison-Wesley, 1970.
9. N.A. Pratten, Review: The Precise Measurement of the Density of Small Samples, *J. Mater. Sci.*, Vol 16, 1981, p 1737-1747.
10. *CRC Handbook of Chemistry and Physics*, R.C. Weast and M.J. Astle, Ed., CRC Press, 1982, p F-11.
11. *Aluminum Standards and Data 1982*, The Aluminum Association, Washington DC., 1982, p 40-41.
12. C.C. Chama, Mechanical Properties of Hot Isostatically Pressed Aluminum-Silicon Castings, *Scr. Metall. Mater.*, Vol 26, 1992, p 1153-1156.
13. *The Elevated-Temperature Properties of Aluminum and Magnesium Alloys*, ASTM, 1960, p 216.
14. *Metals Handbook*, Vol 1, 9th ed., American Society for Metals, 1979, p 152-179.
15. L. Ramqvist, Theories of Hot Pressing, *Powder Metall.*, Vol 9, 1966, p 1-25.
16. L.E. Murr, *Interfacial Phenomena in Metals and Alloys*, Addison-Wesley, 1975, p 185.
17. T.S. Lundy and J.F. Murdock, Diffusion of Al<sup>26</sup> and Mn<sup>54</sup> in Aluminum, *J. Appl. Phys.*, Vol 33, 1962, p 1671-1673.